A spectroscopic study of lanthanide(III) acetate and haloacetates through the correlation of phenomenological intensity parameters and lanthanide induced NMR chemical shifts

D. F. Mullica and **G. A. Wilson**
Department of Chemistry, Baylor University, Waco, TX 76798 (U.S.A.)

(Received June 13, 1990)

Abstract

A series of lanthanide acetate and haloacetate complexes were studied by absorbance spectroscopy and ^{1}H, ^{13}C and ^{17}O NMR in order to determine bonding effects through a correlation of phenomenological intensity parameters with contact shift contributions and calculated polarizabilities of the ligands. A correlation between the ligand polarizability and the oscillator strengths of the hypersensitive transitions for the acetate and haloacetates of Pr^{3+}, Nd^{3+}, Ho^{3+} and Er^{3+} is observed. Also, a linear relationship is observed relating the change in the hypersensitive indicator parameter, Ω_2, to the relative spin density of the nuclei within the ligand having close contact with the lanthanide ion. Such correlations demonstrate a direct relationship between hypersensitive pseudoquadrupole transitions and contact shifts in lanthanide complexes.

Introduction

The absorbance spectra of the lanthanides are characterized by multiple sharp bands of relatively low intensity arising from interconfigurational $4f \rightarrow 4f$ transitions. Their intensities are accounted for by a combination of forced electric dipole and magnetic dipole strengths. While the magnetic dipole strengths are calculated entirely in terms of spectroscopic states constructed within the $4f^n$ electronic configuration, the electric dipole strengths can only be determined by considering mixing of states having opposite parity terms. Over a period of several years, the lanthanides have been investigated in solution and in the condensed phase using a variety of spectroscopic techniques in order to understand the unique properties of these $4f^n$ elements. The puzzling phenomenon of 'hypersensitivity', the extreme sensitivity of certain transitions within the absorbance spectra to the environment of the lanthanide ion, was reported as early as 1930 by Selwood [1]. These transitions have been attributed to a variety of effects which include forced dipoles [2, 3], quadrupole transitions [4, 5], vibronic coupling with the ligands [6], as well as ligand polarization and bonding effects expressed by the nephelauxetic parameter, β, and the basicity of the ligand [7, 8]. Correlations between the $4f \rightarrow 4f$ electric dipole intensities and ligand structure are of significant importance in lanthanide coordination chemistry and in the design of lanthanide optical materials. Most correlations have dealt with the unique diad or tetrad properties exhibited by the lanthanides. Sinha [9] has investigated linear variations in the properties of the lanthanides with the orbital angular quantum number (L, in the ground state) making correlations between lattice constants and bond distances or the number of f-electrons (f^n) of the lanthanides. Investigations have been made by Mason [10], Peacock [11], and Beltyukova *et al.* [12] concerning the phenomenon of hypersensitivity which relate the changes in band intensity to various factors such as the dielectric constant of the solvent, the number of coordinated ligands, as well as the average polarizability and the sum of pK of the ligands.

The role of the $4f^n$ electrons in valency forces has been argued for years and their contribution is considered to be extremely limited. They do, however, play a major role in certain physical properties exhibited by the lanthanides. An imbalance in the orbital angular momentum and spin momentum arises from the addition of electrons into the 4f shell causing the lanthanides to be strongly paramagnetic. Such paramagnetic metal ions are capable of interacting with substrate molecules to generate an additional shift to the NMR signals of their nuclei.

0020-1693/90/$3.50

Certain paramagnetic transition metal complexes produce chemical shifts which give unambiguous structural information. For these compounds, the chemical shifts are determined by electron spin–nuclear spin interactions. The highly paramagnetic lanthanide series is most commonly used in chemical shift studies. The information obtained from shift data can provide a great deal of insight into both the orientation of the ligands around the lanthanide ion and the nature of bonding within the complex.

Electric-dipole transitions occurring with the f^n configuration of the lanthanides are commonly studied by employing the intensity parameterization schemes developed by Judd [13] and Ofelt [14]. These parameters incorporate many interaction mechanisms and carry a great deal of information concerning the origin of hypersensitivity. However, a correlation between the two spectroscopic phenomena, the hypersensitive transitions in the electronic absorbance spectra and the induced chemical shift in nuclear magnetic resonance spectra, has remained uninvestigated. Our investigation examines interactions between the ligands and the metal ion of lanthanide complexes through the correlation of the hypersensitive intensity parameters with ligand polarizabilities and the observed relative spin densities for the ligand nuclei.

Theory and calculations

Absorbance spectra

The oscillator strength of an absorbance band f_{exp}, a quantity directly proportional to the area under the absorption curve, is used as a measure of the intensity and is most commonly expressed in terms of the molar extinction coefficient ϵ, the energy of the transition in wave numbers σ, and the refractive index of the medium η.

$$f_{exp} = \frac{10^3(\ln 10)m_e c^2}{N_A \pi e^2} \frac{9\eta}{(\eta^2+2)^2} \int \epsilon_i(\sigma)\, d\sigma \qquad (1)$$

The electronic transitions of the trivalent lanthanides contain contributions having electric-dipole, magnetic-dipole or electric-quadrupole character. Since electric-dipole transitions are forbidden within an unperturbed f^n configuration, some mixing of opposite parity configurations must occur in order for this mode to make a contribution. For pure electric-quadrupoles, the oscillator strengths are several orders of magnitude too low to account for the observed intensities. The hypersensitive transitions, however, are observed to follow the selection rules for quadrupole radiation ($\Delta J \leqslant 2$, $\Delta L \leqslant 2$, $\Delta S = 0$) and have been referred to as pseudoquadrupole transitions [15–17].

By considering a forced electric dipole mechanism and the excited configurations $4f^{n-1}\,5d$ and $4f^{n-1}\,5g$, Judd [13] and Ofelt [14] independently developed an expression for the oscillator strength of a given transition using three phenomenological parameters, Ω_λ, where λ has values of 2, 4 and 6. These parameters are related to pure electrostatic crystal field effects, vibronic effects or a combination of both effects and are widely used as guiding indices in the analysis of the intensities of f→f transitions. By assuming that the ground state lies at a much lower energy level than the excited configurations $f^{n-1}\,5d$ and $f^{n-1}\,5g$, the Jugg–Ofelt model provides the following expression for the oscillator strength of f→f transitions

$$f_{dip} = \sum_\lambda \frac{8\pi^2 m_e c^2}{3h(2J+1)} \Omega_\lambda \sigma I^{(\lambda)} \qquad (2)$$

where σ is the wave number for the transition (cm^{-1}), Ω_λ are the phenomenological parameters of the Judd–Ofelt equation, and $I^{(\lambda)}$ represents $\langle f^n[LS]J\|U^{(\lambda)}\|f^n[L'S']J'\rangle^2$ where $[LS]$ and $[L'S']$ are the intermediate vectors connected by the unit matrix tensors, $U^{(\lambda)}$. A complete set of $I^{(\lambda)}$ values for the aqueous Ln^{3+} ions have been calculated by Carnall *et al.* [18–21] using the appropriate crystal-field wave functions. The three Ω_λ parameters are commonly obtained from a least-squares fit to oscillator strengths, f_{exp}, obtained using eqn. (1).

Calculation of the magnetic dipole contribution is based on the allowed transitions of $\Delta J = 0$ and $\Delta J = \pm 1$ between the ground state and excited state configurations [22] and is given by

$$f_{mag} = \frac{2\pi}{3hmc} \sigma\eta(2J+1)^{-1}\langle \alpha SLJ\|L+2S\|\alpha SLJ\rangle^2 \qquad (3)$$

NMR induced shifts

Induced NMR chemical shifts originate from the effect of the lanthanide ion on the electron charge distribution of the ligand. These shifts have been attributed to the hyperfine interaction between the electron spin of the central paramagnetic lanthanide ion and the nuclei of the ligands in the complex. The magnitude of these induced chemical shifts are usually quite large and can be related to two independent mechanisms of hyperfine interaction, the contact (Fermi contact, F) and dipolar (pseudo-contact) shift contributions [23–27]. The combination of contact and dipolar shifts constitute an isotropic paramagnetic shift $(\Delta\nu/\nu)^{iso}$. In the case of lanthanide induced shifts, the complex formation shift $(\Delta\nu/\nu)^{comp}$ can be subtracted from the total

observed shift by employing a lanthanum or lutetium reagent as a blank, thus, yielding the isotropic shift.

The contact shift, $(\Delta\nu/\nu)^{con}$, is related to bonding effects in the complex and results from the formation of covalent bonds between the lanthanide ion and the ligands resulting in a redistribution of the electron charge through orbital overlap. The expression for the contact shift given in eqn. (4) is dependent upon the existence of a finite probability of finding the unpaired electron at the nucleus. Its maximum occurs when the probed nucleus in the ligand is in direct contact with the lanthanide ion.

$$(\Delta\nu/\nu)^{con} = (8\pi g_e\beta_e^2)(9kT)^{-1}|\Psi_N(0)|^2\rho_N\langle S_z^G\rangle_M \quad (4)$$

where g_e, β_e and ρ_N are the g factor, Bohr magneton for an electron, and spin-pair density, respectively. $|\Psi_N(0)|^2$ has values of 1.000 for Ψ_{1s} of ^1H nuclei, 8.693 for Ψ_{2s} of ^{13}C nuclei and 14.985 for Ψ_{2s} of ^{17}O nuclei [28]. $\langle S_z^G\rangle_M$ values (reduced shift parameters) have been determined by Golding and Halton [25]. The spin-density transfer can be evaluated by a ratio of the ligand nuclei 1s and 2s wave functions to ^1H Ψ_{1s} from the relationship

$$(\Delta\nu/\nu)^{con} = 2.5\times10^4\left(\frac{\Psi_N(0)^2}{\Psi_H(0)^2}\right)\rho_{rel}\langle S_z^G\rangle_M \quad (5)$$

which can be written as

$$(\Delta\nu/\nu)^{con} = F_N\langle S_z^G\rangle_M \quad (6)$$

where F_N is in frequency units. The component for bonding effects is contained in the hyperfine constant F_N which is very sensitive to the nature of the ligand. The spin–density ratio provides an empirical relationship for the interaction between the ligands and the metal ion in the complex.

The dipolar shift, $(\Delta\nu/\nu)^{dip}$, results from through-space interactions between the paramagnetic lanthanide ion and the ligand nuclei and is present only when the magnetic susceptibility of the central metal ion is anisotropic. For ligand nuclei much further from the lanthanide ion, it is the major mechanism contributing to the total induced shift. Mathematically, the dipolar shift is expressed using geometric terms

$$(\Delta\nu/\nu)^{dip} = D'_M(3\cos^2\theta - 1)r^{-3} \quad (7)$$

where D'_M is derived from crystal field parameters for the appropriate lanthanide ion [24].

Reilley *et al.* [26] have established a method for the dissection of the contact and dipolar contributions from the observed isotropic shift. Their results compared favorably with reported literature values cited in their work and were supported by MO calculations of the ligand spin density distribution and geometric models for the complexes studied [26].

Using fixed values for D'_M and $\langle S_z^G\rangle_M$ [24, 29], the two variables, F_N and G_N (where G_N represents the geometric portion of eqn. (7)), can be determined from a least-squares fit using eqn. (8) in the form (a) for nuclei having a large dipolar shift contribution and in the form (b) for nuclei having a large contact shift contribution.

$$(\Delta\nu/\nu)^{iso} = D'_M G_N + \langle S_z^G\rangle_M F_N \quad (8)$$

$$(\Delta\nu/\nu)^{iso}\langle S_z^G\rangle_M{}^{-1} = \frac{D'_M}{\langle S_z^G\rangle_M}G_N + F_N, \quad (8a)$$

$$(\Delta\nu/\nu)^{iso}D'_M{}^{-1} = G_N + \frac{\langle S_z^G\rangle_M}{D'_M}F_N \quad (8b)$$

Experimental

Stock solutions of Pr^{3+}, Nd^{3+}, Ho^{3+}, Er^{3+}, CH_3COOD, $CH_2ClCOOD$, $CH_2BrCOOD$ and CH_2ICOOD were prepared in D_2O in a glove bag under dry nitrogen. A pH of 2.0 was regulated with DCl and NaOD. Samples used in UV–Vis studies were prepared with constant lanthanide ion concentration whereas those used in NMR studies were prepared with constant ligand concentration.

Absorbance data were collected on an IBM 9430 spectrophotometer at 300 ± 2 K in the range of 900 to 200 nm using 10 mm quartz cells. The near-IR spectra of praseodymium was collected on a Cary-14 spectrophotometer in the range of 1000 to 2500 nm. All spectra were measured while employing a lanthanum blank with the appropriate metal and ligand concentrations. Analyses of the data were performed on a VMS/VAX computer system where the lanthanide ion concentration was confirmed with a least-squares fitting routine using molar absorptivity values reported by Carnall [30] for non-hypersensitive transitions. All UV–Vis spectral data were deconvoluted using an algorithm by Mardquardt [31]. Deconvolution was necessary in order to obtain the oscillator strengths for the $4f\rightarrow4f$ transitions. The transition intensity parameters Ω_2, Ω_4 and Ω_6 were calculated utilizing eqn. (2) after making assignments according to Carnall *et al.* [19].

All NMR data were collected at 300 ± 2 K using a JEOL model FX90Q in the Fourier-transform mode with the following nuclei and observation frequencies: ^1H at 89.55 MHz; ^{13}C at 22.49 MHz; ^{17}O at 12.11 MHz. Acetone was used as an external reference for all three nuclei. Corresponding lanthanum complexes for each lanthanide complex were used as blanks in order to subtract out shifts due to ionic strength, acidity, dilution effects and the chemical shift of the ligand under consideration.

Analyses of the data were performed following corrections of baseline and peak deconvolutions.

Results and discussion

Praseodymium(III) spectra

The f^2 configuration of a free Pr^{3+} ion involves 13 energy levels with the ground term being $^3H_4$. Of these, eight were observed in the near-IR and UV–Vis spectra. The fit of experimental intensity data for Pr(III) using Gaussian envelopes as a basis for integrating the observed absorption bands provided particularly good results. The complex band due to transitions to the $^3F_3$ and $^3F_4$ levels near 6700 cm^{-1} were resolved. This allowed for the determination of the Ω_λ parameters based on eight transitions, two of which are hypersensitive. For the hypersensitive component Ω_2, a value of $103.0(9)\times10^{-20}$ cm^2 (see Table 1) was obtained for the acetate complex which is significantly increased compared to the Pr^{3+} ion in dilute acid solution. The hypersensitive transitions, $^3H_4\rightarrow{}^3F_3$ and $^3H_4\rightarrow{}^3F_4$, in the near-IR have magnetic dipole contributions and are significantly more intense than other possible hypersensitive transitions which contains no magnetic dipole contribution.

Neodyminum(III) spectra

There are 41 energy levels for the f^3 configuration of Nd(III) which arise from spin–orbit splitting of 17 multiplet terms. Several absorbance bands lie in the UV–Vis region due to transitions to excited levels from the $^4I_{9/2}$ ground state. The absorption intensity parameters for the spectra of the neodymium complexes are greatly affected by the hypersensitive transition to the level $^4I_{9/2}\rightarrow{}^4G_{5/2}$ located in the visible region of the spectrum (17 500 cm^{-1}). This transition is overlapped by a less intense hypersensitive transition $^4I_{9/2}\rightarrow{}^2G_{7/2}$ which contributes to the Ω_2 intensity parameter. As many as three Gaussian envelopes were required to account for the oscillator strength of the absorbance bands. A total of 27 transitions for Nd(III) were used in the fitting of the Ω_λ intensity parameters. Values of 0.9(5), 2.0(2) and $4.9(8)\times10^{-20}$ cm^2 were calculated for the hypersensitive parameter (Ω_2) of the acetate, chloroacetate and bromoacetate complexes, respectively (see Table 1). A definite increase in the Ω_2 parameter for the series of ligands is observed. Except for the $^4I_{9/2}\rightarrow{}^4G_{5/2}$ transition, all of the $^4I_{9/2}\rightarrow{}^4G_J$ and $^4I_{9/2}\rightarrow{}^2G_J$ transitions have magnetic dipole contributions.

Holmium(III) spectra

For holmium, 47 multiplet terms arise from the f^{10} configuration which are split into 107 levels due to spin–orbit coupling. The $^5I_8$ level is the ground state. The two transitions, $^5I_8\rightarrow{}^5G_6$ (22 100 cm^{-1}) and $^5I_8\rightarrow{}^3H_6$ (27 700 cm^{-1}), are hypersensitive with $^5I_8\rightarrow{}^5G_6$ being the more intense. Neither of the

TABLE 1. Judd–Ofelt parameters, Ω_λ[a], oscillator strengths, f_{exp}[b], and molar absorptivities, ϵ, calculated from spectroscopic data for $Ln(lig)_3$ in D_2O, where $Ln=Pr^{3+}$, Nd^{3+}, Ho^{3+} and Er^{3+}, and $lig=CH_3COOD$, $CH_2ClCOOD$, and $CH_2BrCOOD$

Ln^{3+}	Ligand	$\langle^{2S+1}L_J\rangle$	ϵ	f_{exp}	Ω_2	Ω_4	Ω_6	*RMS*[c]
Pr^{3+}	CH_3COOD	$\langle^3F_3\rangle$	2.68	3.09	103.0(9)	4.1(1)	4.0(9)	0.5
		$\langle^3F_4\rangle$	4.02	8.89				
Nd^{3+}	CH_3COOD	$\langle^4G_{5/2}\rangle$	3.88	5.46	0.9(50	0.6(3)	14(3)	1.1
		$\langle^2G_{7/2}\rangle$	4.17	2.02				
	$CH_2ClCOOD$	$\langle^4G_{5/2}\rangle$	3.96	5.59	2.0(2)	0.4(2)	14(3)	1.2
		$\langle^2G_{7/2}\rangle$	4.19	2.07				
	$CH_2BrCOOD$	$\langle^4G_{5/2}\rangle$	4.22	5.95	4.9(8)	0.3(2)	12(3)	1.4
		$\langle^2G_{7/2}\rangle$	4.48	2.17				
Ho^{3+}	CH_3COOD	$\langle^5G_6\rangle$	4.25	5.22	0.6(1)	2.4(1)	1.1	1.5
		$\langle^3H_6\rangle$	1.76	2.61				
Er^{3+}	CH_3COOD	$\langle^2H_{11/2}\rangle$	1.75	2.42	0.7(1)	2.4(1)	0.7(1)	2.1
		$\langle^4G_{11/2}\rangle$	2.02	4.26				
	$CH_2ClCOOD$	$\langle^2H_{11/2}\rangle$	1.83	2.45	0.9(1)	2.3(1)	0.7(1)	2.2
		$\langle^4G_{11/2}\rangle$	2.13	4.30				
	$CH_2BrCOOD$	$\langle^2H_{11/2}\rangle$	1.90	2.66	1.1(1)	2.3(1)	0.7(1)	1.5
		$\langle^4G_{11/2}\rangle$	2.50	4.39				

[a]Parameters reported as $\Omega_\lambda\times10^{20}$ ($\lambda=2,4,6$). [b]Oscillator strength $\times10^6$. [c]Root-mean-square $\times10^7$ for fitted parameters.

hypersensitive transitions has a magnetic dipole contribution. The very strong magnetic dipole transition, $^5I_8 \rightarrow {}^3K_8$, occurs within 800 cm^{-1} of $^5I_8 \rightarrow {}^5G_6$. Whereas, $^5I_8 \rightarrow {}^3H_6$ is separated from the two magnetic dipole transitions, $^5I_8 \rightarrow {}^3K_7$ and $^5I_8 \rightarrow {}^3L_9$ by 1500 and 1250 cm^{-1}, respectively. Using the oscillator strengths of the 20 transitions observable in the range 11 000–33 000 cm^{-1}, the intensity parameter Ω_2 was calculated to be $0.6(1) \times 10^{-20}$ cm^2 for the acetate complex, an increase of approximately 50% over that obtained for the Ho^{3+} ion in dilute acid solution (0.36×10^{-20} cm^2) reported by Carnall *et al.* [18].

Erbium(III) spectra

The f^{11} or f^{n-3} configuration is characterized by 17 multiplet terms from which 41 levels arise due to splitting by spin–orbit coupling. The ground state term is $^4I_{15/2}$. The levels are similar to those of the f^3 configuration of neodymium. However, the energy levels for the multiplets are in reverse order and the levels for the erbium configurations occur at higher energies and the number of magnetic dipole transitions are greatly reduced. The hypersensitive transitions for erbium are $^4I_{15/2} \rightarrow {}^2H_{11/2}$ (19 200 cm^{-1}) and $^4I_{15/2} \rightarrow {}^4G_{11/2}$ (26 500 cm^{-1}). The more intense hypersensitive transition, $^4I_{15/2} \rightarrow {}^4G_{11/2}$, is within 1700 cm^{-1} of the strong magnetic dipole transition, $^2K_{15/2}$. A total of 12 transitions observed in the range 11 000–30 000 cm^{-1} were used to obtain values of 0.7(1), 0.9(1) and $1.1(1) \times 10^{-20}$ cm^2 for the Ω_2 intensity parameter (acetate < chloroacetate < bromoacetate, see Table 1). There is only a moderate difference between the Ω_2 values and the Er^{3+} ion in dilute acid solution (0.59×10^{-20}) [18]. The analogous neodymium series has a more pronounced change owing to the difference in its coordination properties and the numerous magnetic dipole transitions.

Shifts in NMR spectra

The isotropic shift data of the nuclei, ^1H, ^{13}C and ^{17}O were measured in Hertz at constant temperature for the acetate complexes of praseodymium, neodymium, holmium and erbium as well as the haloacetate complexes of neodymium and erbium (see Table 2). Due to signal broadening, the ^{17}O shift values for acetate carbonyl could not be obtained and the ^{17}O shifts reported are for the solvent, D_2O. A general trend showing an increase in the frequency for the isotropic ^{13}C shifts in the neodymium and erbium complexes and for the isotropic ^1H shifts in the neodymium complexes is observed, however, the iodoacetate ligands in each series present an anomaly. Regarding the isotropic ^1H shifts for the erbium complexes, no trend is perceived for the series.

The dipolar shift contribution which is dependent upon both the magnetic property and crystal field terms of the lanthanide ion and the structure of the complex is sensitive to variations in the angle θ (eqn. (7)). In most aqueous systems the Ln(III) cation is eight or nine-coordinated. In the case of the latter, absolute magnitudes of lanthanide induced shift values are typically much lower in aqueous solutions than in organic solvents, indicating a distortion from a true tricapped trigonal prismatic geometry [32–34]. The structures for the complexes involving the light lanthanides (La → Eu) differ from those involving the heavy lanthanides (Gd → Lu), i.e. in their mode of complexation. The lanthanide-induced shifts are sensitive to structural alterations in the metal coordination sphere. There is an apparent change from monodentate to bidentate bonding of the acetate across the lanthanide series. For the solution phase, it has been proposed by Sherry and Pascual [35] that these changes result from an expulsion of at least one water molecule from the coordination sphere due to a decrease in the ionic radii. The lighter lanthanide ions are nine-coordinated by the oxygen atoms of three bidentate acetate ligands, and three water molecules, one of these water molecules replaces a bridging oxygen atom from an adjacent acetate ligand which is the case in the solid state.

With reference to the solid state, the M–O bond distances reported by Peters [32] are approximately 2.5 Å for the praseodymium and neodymium complexes (lighter lanthanides) and are approximately 2.4 Å for the heavier lanthanide complexes (holmium and erbium) which is due to the decrease in ionic radii. For the lighter lanthanides the bond angles for oxygen (θ_O) and carbon (θ_C) of R-COO range from 98.15 to 97.53 and 113.87 to 112.25, respectively. The bond angles of the heavy lanthanide acetates have somewhat decreased values ranging from 97.13 to 96.72 for θ_O and from 111.79 to 110.69 for θ_C. This variation in the bond distances and bond angles accounts for the change in the geometric factor, G_N, for light and heavy lanthanide complexes. That is to say, the geometric factor is dependent upon the positions of the ligand nuclei around the metal center.

The contact shift contribution, attributed to through-bond electron spin density transfer, is dependent upon the value of the total spin quantity of the lanthanide ion and the coupling constant of the nucleus which are incorporated into eqn. (4). Then, using the reduced shift parameter constants ($\langle S_z^G \rangle$) from Table 3 and the isotropic shift data, the geometric parameter (G_N) and the contact parameter (F_N) were calculated for the lanthanide

TABLE 2. Shift data in Hertz for [ligand]/[Ln] = 3.0 (Ln = Pr^{3+}, Nd^{3+}, Ho^{3+} and Er^{3+})

Ln^{3+}	Ligand	$^1H_\alpha\ \Delta^{iso}$	$^{13}C_\alpha\ \Delta^{iso}$	$^{13}C_{COO}\ \Delta^{iso}$	$^{17}O_{D_2O}\ \Delta^{iso}$
Pr^{3+}	CH_3COOD	−54.0(3)	−7.1(3)	−0.2(1)	460(1)
Nd^{3+}	CH_3COOD	−611.6(3)	−805.3(3)	−148.7(4)	369(1)
	$CH_2ClCOOD$	−29.8(2)	−31.6(7)	−31.6(6)	559(1)
	$CH_2BrCOOD$	4.5(6)	10.5(9)	−2.5(5)	429(1)
	CH_2ICOOD	5.6(6)	5.1(7)	4.8(3)	260(2)
Ho^{3+}	CH_3COOD	−437.3(5)	−92.4(2)	−115.2(3)	−2809(5)
Er^{3+}	CH_3COOD	201.6(4)	40.9(5)	22.7(4)	−1725(6)
	$CH_2ClCOOD$	286.0(6)	63.0(7)	22.7(6)	−1731(6)
	$CH_2BrCOOD$	198.2(4)	63.0(7)	34.6(5)	−2639(9)
	CH_2ICOOD	85.0(5)	24.6(4)	11.5(4)	−770(2)

TABLE 3. Parameter constants for contact and dipolar contributions of isotropic NMR shifts

Ln^{3+}	$\langle S_z^G\rangle_M$[a]	D'_M[b]	$\langle S_z^G\rangle/D'_M$
Pr	−3.200	−11.89	0.269
Nd	−4.909	−4.77	1.030
Ho	22.500	−36.00	−0.625
Er	15.300	33.04	0.463

[a]The calculated $\langle S_z^G\rangle$ values in units of βH/3kT were obtained from ref. 27.
[b]D'_M values were extrapolated from the resultant data in ref. 30.

acetates employing the appropriate form of eqn. (8). Note in Table 3, the reduced total spin, $\langle S_z^G\rangle_M$, for praseodymium and neodymium have negative values while the heavy lanthanides, holmium and erbium, have positive values. This is due to a change in magnetic properties across the lanthanide series. The parameter F_N presented in Table 4 incorporates the gyromagnetic ratio for the nucleus. Withstanding a few anomalies and in a general sense, the contact parameters (F_N) for each neodymium and erbium complex series tend to decrease.

Employing eqns. (5) and (6), relative spin-pair densities have been calculated from the acquired contact shift parameters of the ligand nuclei. Since the contact shift has only a minimal contribution to more distant ligand nuclei, only relative spin densities of ligand nuclei in close proximity of the lanthanide ion were considered. These are the carbonyl of the acetate and the oxygen of the solvent, see Table 5. The relative spin-density transfer is evaluated by a ratio of $|\Psi_N(0)|^2$ for the nucleus of interest and that of the proton on the ligand, $|\Psi_H(0)|^2$, see eqn. (5). This ratio yields an empirical correlation related to the influence of the metal ion in the complex.

Correlation of parameters

Polarizability and oscillator strengths

Mason [36, 37] considered ligand polarizabilities in the intensity calculations for hypersensitive tran-

TABLE 4. Contact and dipolar contributions of shift data for [ligand]/[Ln] = 3.0

Ln^{3+}	Ligand	^1H		$^{13}C_\alpha$		$^{13}C_{COO}$		$^{17}O_{D_2O}$	
		G_N	F_N	G_N	F_N	G_N	F_N	G_N	F_N
Pr^{3+}	CH_3COOD	−2.0	24.4	−3.82	16.0	−4.50	17.0	5.73	−165.0
Nd^{3+}	CH_3COOD	−2.0	91.0	−3.82	34.1	−4.50	35.1	5.73	−143.4
	$CH_2ClCOOD$	−2.0	3.1	−3.82	6.0	−4.50	11.9	5.73	−171.5
	$CH_2BrCOOD$	−2.0	−2.9	−3.82	2.1	−4.50	2.9	5.73	−185.0
	CH_2ICOOD	−2.0	−10.0	−3.82	2.5	−4.50	3.2	5.73	−60.0
Ho^{3+}	CH_3COOD	−1.4	−21.7	−2.63	1.0	−5.90	−14.6	6.96	−62.5
Er^{3+}	CH_3COOD	−1.4	16.2	−2.63	8.4	−5.90	14.3	6.96	−123.1
	$CH_2ClCOOD$	−1.4	21.7	−2.63	8.3	−5.90	14.3	6.96	−144.0
	$CH_2BrCOOD$	−1.4	15.9	−2.63	8.3	−5.90	14.9	6.96	−184.0
	CH_2ICOOD	−1.4	8.6	−2.63	7.3	−5.90	13.4	6.96	−64.9

TABLE 5. Relative spin density of $^{13}C_{COO}$ and $^{17}O_{D_2O}$ nuclei

Ln^{3+}	Ligand	$^{13}C_{COO}$	$^{17}O_{D_2O}$
Pr^{3+}	CH_3COOD	3.0	−54.4
Nd^{3+}	CH_3COOD	1.2	−11.8
	$CH_2ClCOOD$	2.0	−473.0
	$CH_2BrCOOD$	4.3	−513.3
	CH_2ICOOD	6.3[a]	–
Ho^{3+}	CH_3COOD	0.65	−5.2
Er^{3+}	CH_3COOD	0.63	−10.2
	$CH_2ClCOOD$	0.62	−11.9
	$CH_2BrCOOD$	0.62	−15.2
	CH_2ICOOD	0.66	−19.6[a]

[a]Interpolated from linear relation of polarizability and spin density.

sitions to account for dynamic contributions made by the perturbed ligands. Jezowska-Trzebiatowska *et al* [38] investigated polarizability effects on the spectra of europium(III) compounds in non-aqueous solutions. Assuming the ligands to be isotropic, they showed a proportionality between the oscillator strengths and the polarizability of the ligands. The polarizability of the ligands can be express in terms of the mean molar refractivities by a simple relation

$$\alpha = 0.3964 \times 10^{-24} R_\infty \quad (9)$$

where α has units of cm^{-3} and R_∞ is the mean molar refractivity in the infinite wavelength limit

$$R_\nu = \frac{\eta_\nu^2 - 1}{\eta_\nu^2 + 2} \frac{M}{d} \quad (10)$$

with M as molecular weight, d as density and η_ν as refractive index at wavelength ν.

The oscillator strengths of the hypersensitive pseudoquadrupole transitions for neodymium and erbium are observed to increase as the polarizability of the ligand increases. Regressional analysis of oscillator strengths of the hypersensitive transitions versus the ligand polarizabilities calculated from eqns. (9) and (10) for the acetate, chloroacetate and bromoacetate complexes of neodymium and erbium, revealed linearity. For the two hypersensitive transitions of neodymium the linear relationships yielded angular coefficients and intercepts of 0.110 and 3.704 for $\langle {}^4G_{5/2} \rangle$, and 0.030 and 2.766 for $\langle {}^2G_{7/2} \rangle$. The correlation coefficients (ρ^2) are 0.982 and 0.977, respectively. Regarding the two hypersensitive transitions of erbium, angular coefficients and intercepts of 0.029 and 3.788 for $\langle {}^4G_{11/2} \rangle$ and 0.053 and 1.562 for $\langle {}^2H_{11/2} \rangle$ were obtained with correlation coefficients of 0.986 and 0.922, respectively.

Hypersensitivity and spin density

A relationship between the hypersensitive pseudoquadrupole transitions of the lanthanide ions with the contact shifts measured from the induced shifts of the ligand nuclei exists through the electron density interactions which occur between the f-orbitals of the metal ions. Through angular overlap, a perturbation is produced which can be observed by correlating the change of the hypersensitive parameter, Ω_2, with the relative spin density on the ligand nuclei. The lanthanide acetate complexes show such a correlation (see Fig. 1) between $\Delta\Omega_2$ and the $^{17}O_{D_2O}$ nuclei of the solvent. Linear regressional analysis yields an angular coefficient of -272.7 Hz/cm^2 and intercept of 85.18 Hz ($\rho^2 = 0.998$). A linear correlation is also observed when plotting the relative spin density for the $^{13}C_{COO}$ nuclei against $\Delta\Omega_2$ for the acetate and haloacetate complexes of the light lanthanide, Nd^{3+} (see Fig. 2). A least-squares analysis provided an angular coefficient of 0.712 Hz/cm^2 and intercept of 1.010 Hz ($\rho^2 = 0.991$). As shown in Fig. 3 for the heavy lanthanide, Er^{3+}, Ω_2 correlates linearly with the $^{17}O_{D_2O}$ nuclei of the solvent having an angular

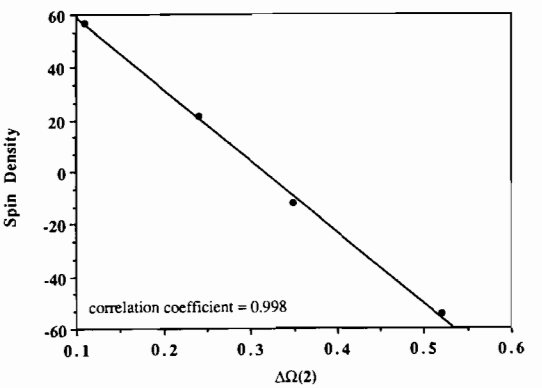

Fig. 1. Plot of $^{17}O_{D_2O}$ spin density vs. change in the Ω_2 intensity parameter for acetate complexes of Pr(III), Nd(III), Ho(III) and Er(III).

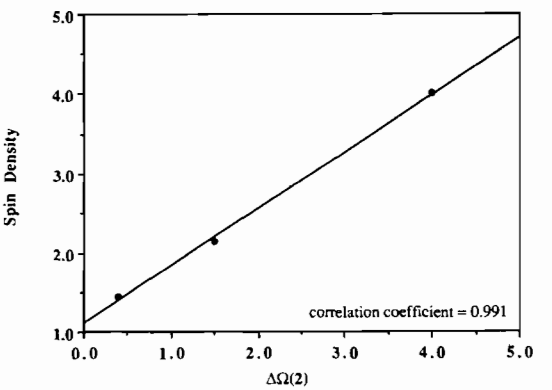

Fig. 2. Plot of $^{13}C_{COO}$ spin density vs. change in Ω_2 intensity parameter for neodymium(III) complexes.

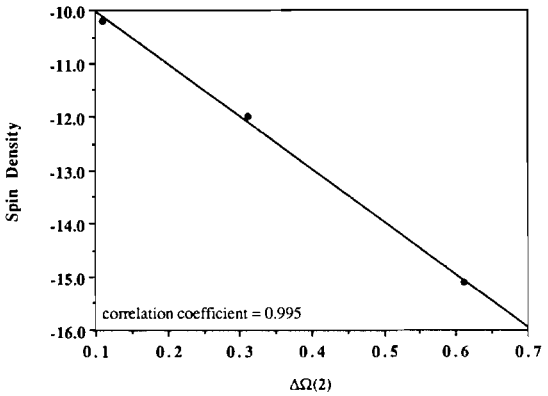

Fig. 3. Plot of $^{17}O_{D_2O}$ spin density vs. change in Ω_2 intensity parameters for erbium(III) complexes.

coefficient of -10.079 Hz/cm^2 and an intercept of -8.97 Hz ($\rho^2 = 0.995$).

Angular coefficients obtained from the hypersensitive parameter and spin density correlations provide evidence that a definite relationship between electron density perturbation of the ligand nuclei and the lanthanide ion exists. Non-zero intercepts can be attributed to deviations of isotropic shifts in relationship to the chemical shifts of the pure ligand.

By utilizing NMR data of a series of analogous complexes, it is possible to determine the phenomenological parameter for hypersensitivity, Ω_2. For example, calculation of the transition intensities for the lanthanide iodoacetate complexes was not attained due to an intense broad band in the UV–Vis spectra which resulted from the presence of free iodine. However, by using interpolated contact shift values for the iodoacetate complexes, the Ω_2 intensity parameters were calculated for the neodymium and erbium iodoacetate complexes, 7.85 and 1.40 cm^2, respectively. Using this method, calculation of theoretical oscillator strengths is also possible for a complex which provided an insufficient number of transitions in UV–Vis spectra.

Conclusions

A direct correlation has been made between the Judd–Ofelt intensity parameter (Ω_2) which is an indicator of the effect of hypersensitivity and the hyperfine coupling parameter (F_N) which accounts for polarizability and covalency effects of the ligand. The angular coefficients from the linear correlations provide a means by which the two spectroscopic phenomena can be related, and provide a measure the covalency contribution within the lanthanide–ligand bonds (approximately 7–10%). Further, the magnetic properties of the lanthanides play an important role in the NMR induced shifts, in terms of the dipolar shift. The magnetic dipole transitions of the lanthanides observed in the UV–Vis spectroscopic studies may also make a contribution to the LSR effect. The magnitude of the change in the Ω_2 intensity parameter associated with hypersensitivity is proportional to the number of magnetic dipole transitions allowed for the lanthanide ion and to their intensities as well as to the separation between the energy levels of the magnetic dipole transitions and those of the hypersensitive transitions.

From the obtained relationships, calculations of approximate intensity values are possible from NMR shift data and a knowledge of the atomic coordinates of a series of complexes involving analogous ligands. More importantly, NMR shifts which are not readily obtainable for the solid state may be determined for a series of analogous crystalline complexes from intensity parameters calculated from the absorbance spectra.

Acknowledgements

Acknowledgement is made to the donors of the Petroleum Research Fund (Grant No. 18633-AC3) administered by the American Chemical Society, and to The Robert A. Welch Foundation (Grant No. AA-668) for partial support of this research.

References

1 P. W. Selwood, *J. Am. Chem. Soc., 52* (1930) 4308.
2 M. F. Reid and F. S. Richardson, *J. Chem. Phys., 79* (1983) 5735.
3 M. F. Reid and F. S. Richardson, *J. Chem. Phys., 88* (1984) 3586.
4 J. H. Van Vleck, *J. Phys. Chem., 41* (1936) 67.
5 W. T. Carnall, D. M. Gruen and R. L. McBeth, *J. Phys. Chem., 62* (1962) 438.
6 D. M. Gruen and C. W. DeKock, *J. Chem. Phys., 45* (1966) 455.
7 D. E. Henrie, R. L. Fellows and G. R. Choppin, *Coord. Chem., Rev., 18* (1976) 199.
8 R. L. Fellows and G. R. Choppin, *J. Coord. Chem., 4* (1974) 79.
9 S. P. Sinha, in S. P. Sinha (ed.), *Proc. NATO Advanced Study Institute on Systematics and the Properties of the Lanthanides*, Reidel, Dordrecht, 1982, Ch. 3.
10 S. F. Mason, *J. Mol. Struct., 60* (1980) 363.
11 R. D. Peacock, *Struct. Bonding (Berlin), 22* (1974) 83.
12 S. V. Beltyukova, N. A. Nazarenko and N. S. Poluektov, in B. Jezowska-Trzebiatowska, J. Legendziewicz and W. Strek (eds.), *Rare Earths Spectroscopy*, World Scientific, Philadelphia, PA, 1984, p. 162.
13 B. R. Judd, *Phys. Rev., 127* (1962) 750.
14 G. S. Ofelt, *J. Chem. Phys., 37* (1962) 511.

15 C. K. Jørgensen and B. R. Judd, *Mol. Phys., 8* (1964) 281.
16 B. R. Judd, *J. Chem. Phys., 4* (1966) 839.
17 J. L. Ryan and C. K. Jørgensen, *J. Phys. Chem., 70* (1966) 2845.
18 W. T. Carnall, P. R. Fields and B. G. Wyborne, *J. Chem. Phys., 49* (1968) 4412.
19 W. T. Carnall, P. R. Fields and K. Rajnak, *J. Chem. Phys., 49* (1968) 4424.
20 W. T. Carnall, P. R. Fields and K. Rajnak, *J. Chem. Phys., 49* (1968) 4443.
21 W. T. Carnall, P. R. Fields and K. Rajnak, *J. Chem. Phys., 49* (1968) 4447.
22 L. J. F. Broer, C. J. Gorter and J. Hoogschagen, *Physica, 11* (1945) 231.
23 A. Abraham and B. Bleaney, *Electron Paramagnetic Resonance of Transition Ions*, Clarendon, Oxford, 1970.
24 B. Bleaney, C. M. Dobson, B. A. Levine, R. B. Martin, R. J. P. Williams and A. B. Xavier, *J. Chem. Soc., Chem. Commun.*, (1972) 791.
25 R. M. Golding and M. P. Halton, *Aust. J. Chem., 25* (1972) 2577.
26 C. N. Reilley, B. W. Good and J. F. Desreux, *Anal. Chem., 47* (1975) 2110.
27 J. Reuben and G. A. Elgavish, in K. A. Gschneidener, Jr. and L. R. Eyring (eds.), *Handbook on the Physics and Chemistry of Rare Earths*, Vol. 4, North-Holland, New York, 1979, Ch. 38.
28 C. N. Reilley, B. W. Good and R. D. Allendoerfer, *Anal. Chem., 48* (1976) 1446.
29 R. M. Golding and P. Pyykkö, *Mol. Phys., 26* (1973) 1389.
30 W. T. Carnall, in K. A. Gschneidner and L. Eyring (eds.), *Handbook on the Physics and Chemistry of Rare Earths*, Vol. III, North-Holland, New York, 1979.
31 W. Mardquardt, *J. Soc. Ind. Appl. Math., 11* (1963) 431.
32 J. A. Peters, *J. Magn. Reson., 68* (1986) 240.
33 M. C. Favas, D. L. Kepert, B. W. Skelton and A. H. White, *J. Chem. Soc., Dalton Trans.,* (1980) 454.
34 L. A. Aslanov, I. K. Abdul'minev, M. A. Porai-Koshits and V. I. Ivanov, *Dolklady Akademii Nauk SSSR, 205* (1972) 343.
35 A. D. Sherry and E. Pascual, *J. Am. Chem. Soc., 99* (1977) 5871.
36 S. F. Mason, *Accnt. Chem. Res., 12* (1979) 55.
37 S. F. Mason, *Struct. Bonding (Berlin), 39* (1980) 43.
38 B. Jezowska-Trzebiatowska, J. Legendziewicz and W. Strek, *Inorg. Chim. Acta, 95* (1984) 157.